Progress In Electromagnetics Research M, Vol. 106, 127–137, 2021

An Integro-Differential Approach for Eddy Currents Computation in Structures Having Heterogeneous Dimensions

Lyes Aomar* **and Hicham Allag**

Abstract—The aim of this paper is to develop a hybrid modeling approach based on direct coupling between the finite element method (FEM) and the partial element equivalent circuits method (PEEC). Through this FEM-PEEC approach, we can efficiently compute the three-dimensional eddy current distribution created by a rectangular coil (exciting coil) in conductive and magnetic structures having heterogeneous dimensions. Magnetic field created by the rectangular coil is given by calculating quasi-static Green's function integrals. In goal to construct rectangular coil, the calculation is made for elementary parallelepipedic conductors oriented respectively in x and y directions. By this manner, three possible configurations are proposed and compared to show errors, especially in corners. By only meshing the active parts of the domain (without air region), we confirm through the issued results that the proposed methodology contributes to accelerate the execution time while maintaining the precision. The obtained results are validated with the numerical ones by 3D FEM (Flux 3D Software).

1. INTRODUCTION

Eddy current distribution in structures having heterogeneous dimensions is a crucial step in the design or the testing process of electromagnetic devices [1], such as nondestructive testing (NDT), problems on carbon fiber composite materials (CFCM) [2], wireless power transfer (WPT) [3], motion sensors (MS) [4], and robotic induction heating system (RIHS) as shown in Figure 1(a) [5, 6]. During recent years, many researches and developments in computing methods to model or to predict the eddy current distribution in different parts of complex devices comprising solid conductors and ferromagnetic regions are largely investigated [7–14]. The succeeded computing is the fastest without losses in physical information. This particularity is very important to enable a broad exploratory investigation of the testing and design space [11, 15]. The differential approach, such as FEM method, allows modeling of complex devices, but this kind of methods is computationally expensive especially with structures containing a large number of conductors and having heterogeneous dimensions. In other words, the mesh needs to be refined around those conductors to take into accounts the fast variation of the magnetic field [16, 21]. Meshing the surrounding air space can be avoided using the integral approach with its Coulombian or Amperian considerations [22, 25]. The PEEC method is based on the Amperian one, by considering currents dipoles as elementary conductors. Each conductor can be subdivided into a plurality of elementary conductors for considering electromagnetic local phenomena [26–30]. In PEEC consideration, resistances, self and mutual inductances of the elementary parallelepipedic conductors can be analytically calculated permitting less memory and computational effort than the FEM method. However, taking into account ferromagnetic regions is very complicated and can be part of several interesting PEEC solutions [12, 31, 32].

The main aim of this work is the development of an Integro-Differential formulation able to model structures with heterogeneous dimensions. The particularity is to simulate the eddy currents in thin

Received 26 August 2021, Accepted 7 December 2021, Scheduled 19 December 2021
* Corresponding author: Lyes Aomar (aomarlyes@univ-jijel.dz).
The authors are with the Electrical and Industrial Electronic Laboratory L2EI, University of Jijel, Algeria.

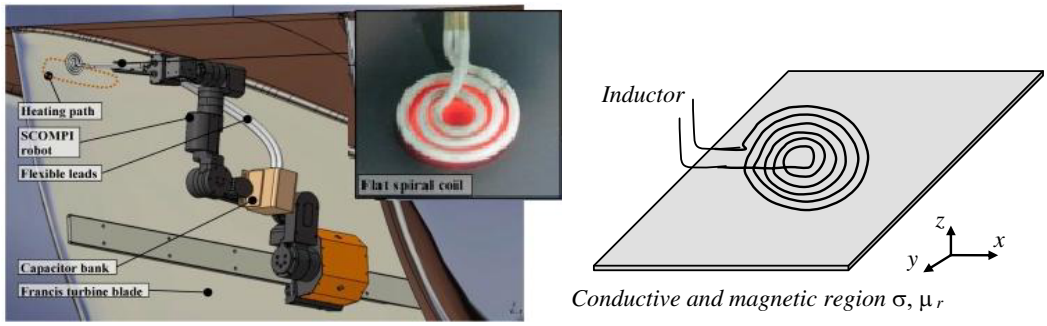

(a) (b)

Figure 1. (a) Induction heat treatment system [5]. (b) Electromagnetic model.

plates with implementing magnetization and current effects and then calculate the integral results among 2D triangular finite elements. A regular mesh of exciting coil is generated by PEEC method considerations. By this manner, we also benefit from the advantages of both methods (PEEC and FEM), such as reduced computation time, taking into account complex conductors, and considering magnetic materials. A case study, as given in Figure 1(b), is used to introduce the modeling approach and to assess its effectiveness. The simulation results of the adopted approach will be compared subsequently with those numerical using a purely numerical approach based on finite elements (3D Flux software).

2. INTEGRO-DIFFERENTIAL FORMULATION

Generally, in the presence of magnetic materials, eddy current problem in the thin plate is modeled using the electric vector potential $\overrightarrow{T}$ respecting the governing equation [12, 33]

$$\overrightarrow{rot}\left(\frac{1}{\sigma}\overrightarrow{rot}\overrightarrow{T}\right) = -j\,\omega\,\mu_0\,\mu_r\overrightarrow{H} \tag{1}$$

The eddy current density $\overrightarrow{J_e}$

$$\overrightarrow{J_e} = \overrightarrow{rot}\overrightarrow{T} \tag{2}$$

The eddy currents are assumed to flow tangentially to the plate.

At any point $P(x, y, z)$, the total magnetic field is given:

$$\overrightarrow{H}(P) = \overrightarrow{H_c}(p) + \overrightarrow{H_i}(p) + \overrightarrow{H_m}(p) \tag{3}$$

where $\overrightarrow{H_c}(p)$: Magnetic field created by the exciting coil. $\overrightarrow{H_i}(p)$: Magnetic field induced by the eddy currents in the thin plate. $\overrightarrow{H_m}(p)$: Magnetic field due to magnetic substance.

2.1. Magnetic Field from the Excitation Coil

In this study, the magnetic field will be calculated from the elementary parallelepipedic conductors forming a final exciting coil situated in XY plane. Consequently, the elementary inclined conductor can be composed of two ones situated at X and Y axes, as shown in Figure 2. The corresponding parallelepipedic conductors carry respectively J_x and J_y current densities. From this situation, we try to calculate the magnetic vector potential and the magnetic field at any point position of freespace [23].

The A_x and A_y magnetic vector potential components for the two conductors carrying respectively J_x and J_y current densities are expressed as [22, 23]:

$$A_x = \frac{\mu_0}{4\pi}\int_{-c1}^{c1}\int_{-b1}^{b1}\int_{-a1}^{a1}\frac{J_x}{|\vec{r}_1 - \vec{r}\,'|}dx_1dy_1dz_1 \tag{4}$$

$$A_y = \frac{\mu_0}{4\pi}\int_{-c2}^{c2}\int_{-b2}^{b2}\int_{-a2}^{a2}\frac{J_y}{|\vec{r}_2 - \vec{r}\,'|}dx_2dy_2dz_2 \tag{5}$$

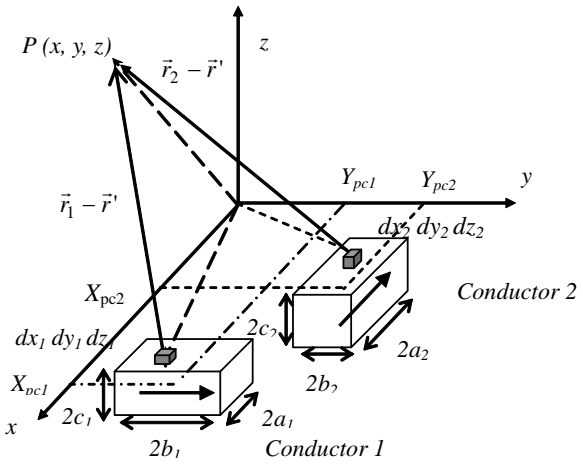

Figure 2. Calculation principle from elementary conductors.

where respectively

$$\left|\overrightarrow{r_1} - \overrightarrow{r'}\right| = \sqrt{(x_1 - x')^2 + (y_1 - y')^2 + (z_1 - z')^2} \tag{6}$$

$$\left|\overrightarrow{r_2} - \overrightarrow{r'}\right| = \sqrt{(x_2 - x')^2 + (y_2 - y')^2 + (z_2 - z')^2} \tag{7}$$

The Magnetic flux densities and field are given by:

$$\overrightarrow{B} = \overrightarrow{Rot}\,\overrightarrow{A} \tag{8}$$

$$\overrightarrow{B} = \mu_0\,\overrightarrow{H} \tag{9}$$

After all integration, the expressions of the three components of the magnetic field are given by intermediary variables U, V, and W:

$$H_{nx} = -\frac{1}{\mu_0}\frac{\partial A_y}{\partial z} = \frac{1}{4\pi}\sum_{i=0}^{1}\sum_{j=0}^{1}\sum_{k=0}^{1}(-1)^{i+j+k}\,\psi_{nx}(U, V, W) \tag{10}$$

$$H_{ny} = \frac{1}{\mu_0}\frac{\partial A_x}{\partial z} = \frac{1}{4\pi}\sum_{i=0}^{1}\sum_{j=0}^{1}\sum_{k=0}^{1}(-1)^{i+j+k}\,\psi_{ny}(U, V, W) \tag{11}$$

$$H_{nz} = \frac{1}{\mu_0}\left(\frac{\partial A_y}{\partial x} - \frac{\partial A_x}{\partial y}\right) = \frac{1}{4\pi}\sum_{i=0}^{1}\sum_{j=0}^{1}\sum_{k=0}^{1}(-1)^{i+j+k}\,\psi_{nz}(U, V, W) \tag{12}$$

With

$$\psi_{nx}(U_1, V_1, W_1) = J_x\left(U_1 \ln(r_1 - V_1) + V_1 \ln(r_1 - U_1) + W_1\, tg^{-1}\left(\frac{U_1 V_1}{W_1 r_1}\right)\right) \tag{13}$$

$$\psi_{ny}(U_2, V_2, W_2) = J_y\left(-U_2 \ln(r_2 - V_2) + V_2 \ln(r_2 - U_2) - W_2\, tg^{-1}\left(\frac{U_2 V_2}{W_2 r_2}\right)\right) \tag{14}$$

$$\begin{aligned}\psi_{nz}(U, V, W) = {} & J_x\left(W_1 \ln(r_1 - V_1) - V_1 \ln(r_1 - W_1) - U_1\, tg^{-1}\left(\frac{W_1 V_1}{U_1 r_1}\right)\right) \\ & + J_y\left(U_2 \ln(r_2 - W_2) + W_2 \ln(r_2 - U_2) - V_2\, tg^{-1}\left(\frac{U_2 W_2}{V_2 r_2}\right)\right)\end{aligned} \tag{15}$$

where

$$U_1 = x - (-1)^i a_1 - X_{pc1}, \quad V_1 = y - (-1)^j b_1 - Y_{pc1}, \quad W_1 = z - (-1)^k c_1, \quad r_1 = \sqrt{U_1^2 + V_1^2 + W_1^2}$$

$$U_2 = x - (-1)^i a_2 - X_{pc2}, \quad V_2 = y - (-1)^j b_2 - Y_{pc2}, \quad W_2 = z - (-1)^k c_2, \quad r_2 = \sqrt{U_2^2 + V_2^2 + W_2^2}$$

a_i, b_i and c_i: are elementary conductor I dimensions. X_{pci}, Y_{pci} and Z_{pci}: are the center's coordinates of elementary conductor i.

Finally, we can generalize this concept to calculate the magnetic field created by the rectangular coil.

$$H_{x\,coil} = \sum_{n=1}^{4} H_{xn} \tag{16}$$

$$H_{y\,coil} = \sum_{n=1}^{4} H_{yn} \tag{17}$$

$$H_{z\,coil} = \sum_{n=1}^{4} H_{zn} \tag{18}$$

2.2. Magnetic Field Created by the Eddy Current

We use the Biot-Savart law to calculate the magnetic field created by eddy currents at any point P of the mesh elements. So we obtain:

$$\overrightarrow{H_i}(p) = \frac{e}{4\pi} \int\limits_{S_m} \frac{\overrightarrow{J_e} \times \overrightarrow{r}}{r^3} dS_m \tag{19}$$

where e: is the thickness of the conductive plate. $\overrightarrow{r}$: is the vector between the integration point and P, $\overrightarrow{r} = (x_i - x_p)\,\overrightarrow{e_x} + (y_i - y_p)\,\overrightarrow{e_y}$.

2.3. Magnetic Field Issued from Magnetic Substance Hm

At any point P, as shown in Figure 3, the reduced magnetic scalar potential around magnetic volume is given: [13, 18]

$$\varphi_m(p) = -\frac{1}{4\pi} \int\limits_{V} \overrightarrow{M}\, \overrightarrow{grad}\left(\frac{1}{r}\right) dV \tag{20}$$

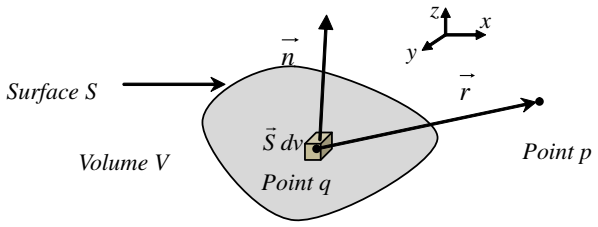

Figure 3. Notations used to calculate H_m.

We use the expression of the magnetic field created by a magnetic volume [33, 34]:

$$\overrightarrow{H_m}(P) = -\frac{1}{4\pi} \int\limits_{V} \overrightarrow{grad}\left(\frac{\overrightarrow{M} \cdot \overrightarrow{n}}{r}\right) dS \tag{21}$$

$$\overrightarrow{r} = (x_q - x_p)\,\overrightarrow{e_x} + (y_q - y_p)\,\overrightarrow{e_y} + (z_q - z_p)\,\overrightarrow{e_z}$$

For a magnetized field in thin plate, represented by a surface S_m and thickness e, we can deduce:

$$\overrightarrow{H_m}(P) = -\frac{e}{4\pi} \int\limits_{S} \overrightarrow{grad_s}\left(\frac{\overrightarrow{M}\,.\,\overrightarrow{n}}{r}\right) dS \tag{22}$$

In this case $\overrightarrow{r} = (x_q - x_p)\,\overrightarrow{e_x} + (y_q - y_p)\,\overrightarrow{e_y}$.

2.4. Governing Electromagnetic Problem

To compute the eddy current produced by the conductor coil, we integrate all the contributed quantities in only one system equations, as follows:

$$\begin{cases} \overrightarrow{rot}\left(\frac{1}{\sigma}\overrightarrow{rot}\overrightarrow{T}\right) + j\,\omega\,\mu_0\,\mu_r\frac{e}{4\pi}\int\limits_{S_m}\frac{\overrightarrow{J_e}\times\overrightarrow{r}}{r^3}dS_m - \frac{e}{4\pi}\int\limits_{S}\overrightarrow{grad_s}\left(\frac{\overrightarrow{M}\,.\,\overrightarrow{n}}{r}\right)dS = -j\,\omega\,\mu_0\,\mu_r\overrightarrow{H_0} \\ \overrightarrow{J_e} = \overrightarrow{rot}\;\overrightarrow{T} \\ \overrightarrow{M} = j\frac{(\mu_r - 1)}{\omega\,\mu_0\,\mu_r\,\sigma}\overrightarrow{rot}\left(\overrightarrow{rot}\overrightarrow{T}\right) \end{cases} \tag{23}$$

Together with the relation $(\mathrm{div}(\overrightarrow{J_e}) = 0)$ and appropriate boundary conditions for the normal component of the current density vector on the conductor surface, the last equation defines a unique solution for the current density vector $\overrightarrow{J_e}$. This Integro-Differential equation (Equation (23)) for the current density vector does not require introducing the scalar electric potential.

2.5. Electromagnetic Problem Calculation Principle

To solve Equation (19) numerically, we split thin plate (conductive and ferromagnetic region) into a set of triangular elements and conductor coil into a set of elementary parallelepiped conductors, as shown in Figure 4.

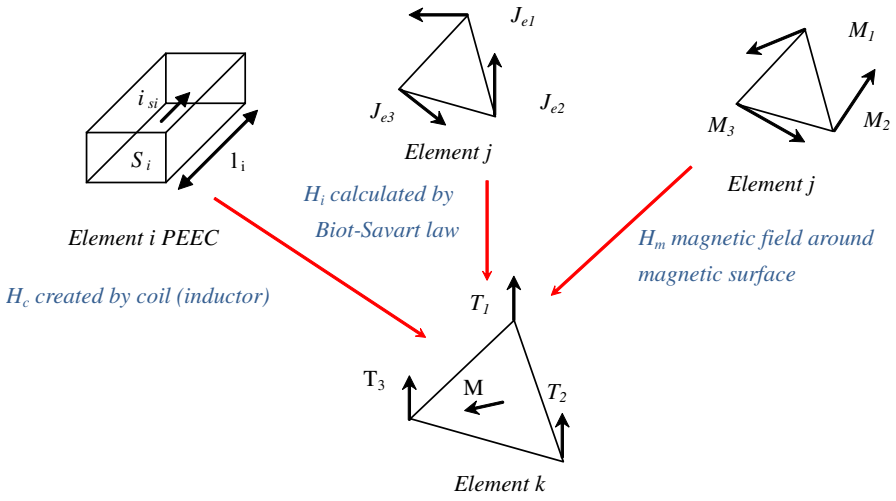

Figure 4. Contribution of all mesh elements.

3. MODEL VALIDATION

3.1. Model Parameters

We consider a fundamental application, as shown in Figure 1(b). The conductive coil, which is placed below a magnetic or non-magnetic conductive plate. The characteristics of the model are listed in Table 1.

3.2. Simulation Results

3.2.1. Magnetic Field Simulation

We can propose three possible configurations for modeling rectangular coils, composed of elementary parallelepiped segments as shown in Figure 5. The dimensions of each elementary conductor are

Table 1. Model parameters.

Symbol	Quantities	Values
I	value of excitation current	1 A
f	frequency of voltage source	50 Hz
μ_r	Permeability of the thin plate	50 H/m
ρ	Electrical resistivity of the thin plate	10.4 10^{-8} Ωm
L_x	Length of the thin plate	200 mm
L_y	Width of the thin plate	200 mm
E	Thickness of the thin plate	1.5 mm
l_x	Length of coil	50 mm
l_y	Width of coil	50 mm
l_z	Height of coil	1.7 mm
Lar	Thickness of coil	5 mm
N	Number of turns of the coil	240
γ	Distance between coil and thin plate in z-direction	2.5 mm

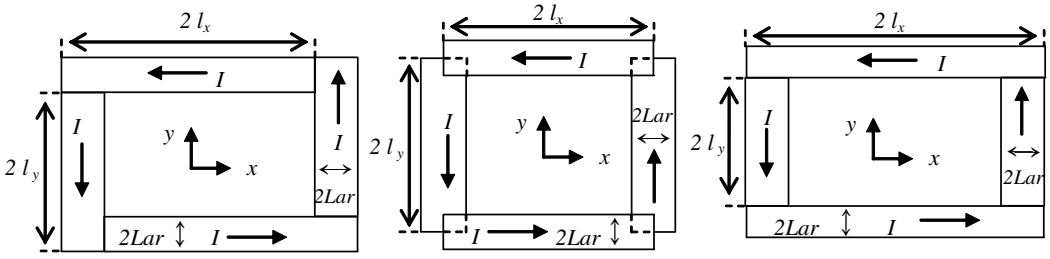

Figure 5. Top view of three possible modeling configurations of the rectangular coil.

$(2l_x \times 2l_y \times 2l_z)$.

In following, we present simulation results of magnetic flux density in XY plane immediately on the top of the coil, at exactly 0.1 mm.

We can see from Figure 6 that the magnetic field reproduces the shapes of the three proposed configurations modeling rectangular coil. In 2D view of Figure 7, all the configurations have clearly confirmed the robustness of our model. Notice that all the calculation results are obtained with great computing rapidity. The three precedent configurations of the coil are different, especially at the corners inducing the edge effect problems. To view that effect, we have chosen to show the difference between

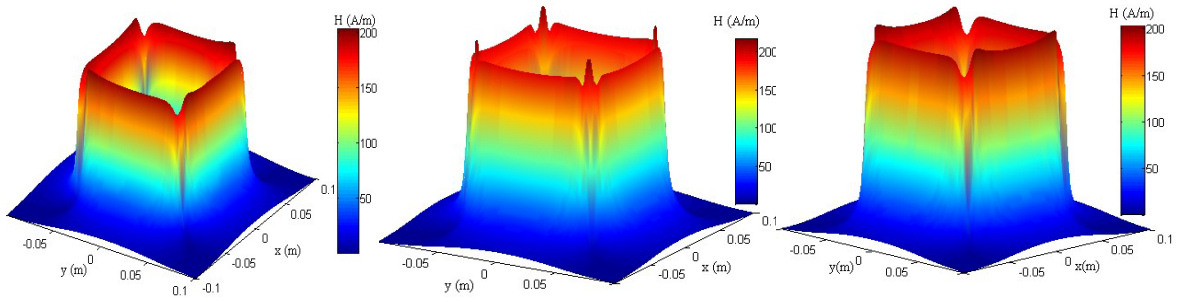

Figure 6. Magnetic field in XY plane, 3D view for three possible configurations.

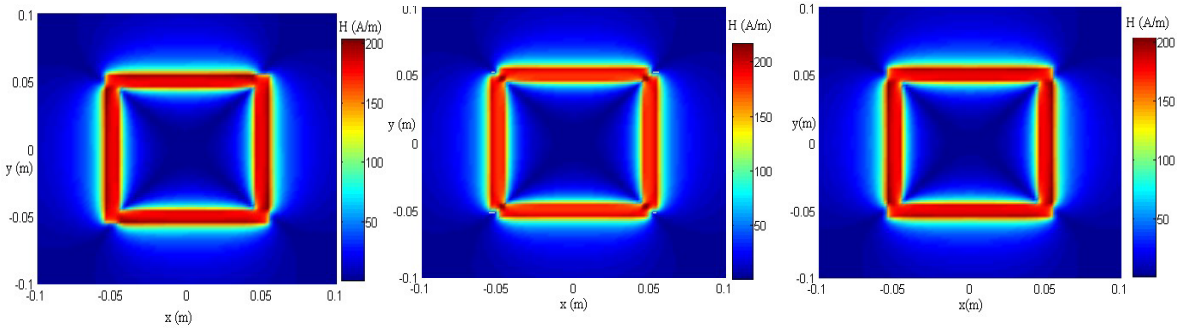

Figure 7. Magnetic field in XY plane, 2D view for three possible configurations.

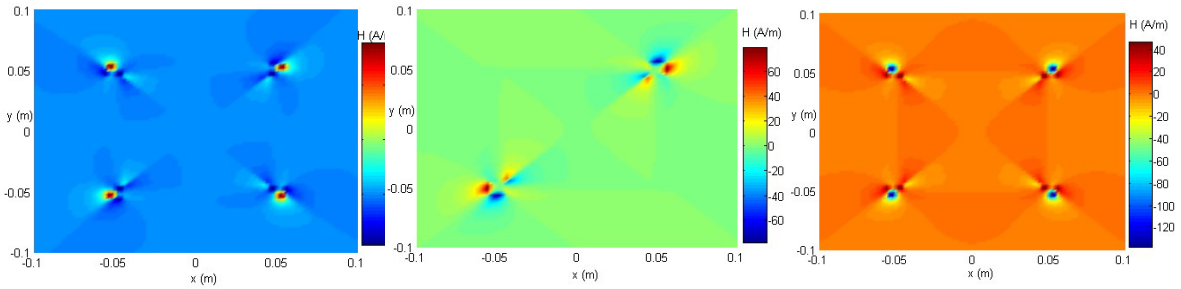

Figure 8. Magnetic field difference in XY plane, 2D view for three configurations. (a) Between configurations a and b. (b) Between configurations b and c. (c) Between configuration a and c.

earlier calculations of magnetic flux density in the XY plane for the cited configurations.

The three figures in Figure 8, ((a), (b), and (c)), present respectively the difference between configurations (a)–(b), (b)–(c), and (a)–(c) subtraction results. It is evident to have the most important value at symmetrical corner zones. These differences will be insignificant as long as the width side of the cross section will be reduced.

4. EDDY CURRENTS SIMULATION

After simulation of the FEM-PEEC model, we now validate the results. From Figure 9, we observe a good distribution of eddy current curves on the thin plate, representing the shape of the excitation coil (rectangular shape). In Figure 9 and Figure 10, we test the accuracy of FEM-PEEC approach by the comparison of our simulation results with those from 3D finite element method (Flux 3D Software).

The particularity of the finite elements method, when we use an adapted mesh aiming to refine regions in a relevant way, will generate an expensive calculation, which forces us to go through techniques for optimizing the relationship between the precision of the results and the simulation costs. In Table 2, we compare computing time taken by the two methods to obtain similar results (difference of 0.7%).

When using electromagnetic nondestructive evaluation (NDE) [15], the measurement signal received by the probe coil is determined by an error related to the operating parameters being inspected. Invariant pattern recognition techniques have been investigated to make NDE signals insensitive to operational fluctuations and to store or restore crack information. For a tilted probe coil, the distribution of eddy current is stronger when the coil is closer to the conductive plate. Our calculation code allows us to see the tilting effect of inductors flexibly, based on the same principle of spatial rotations and Euler's transformation matrix presented in [22]. Figure 10 shows the coil inclines effect on the currents induced in the conductive plate for all of the cited forms of inductors.

Lift-off is the change in impedance that occurs when the distance between the coil probe and the conductive plate changes. The lift-off is stronger near the probe because the magnetic field is stronger

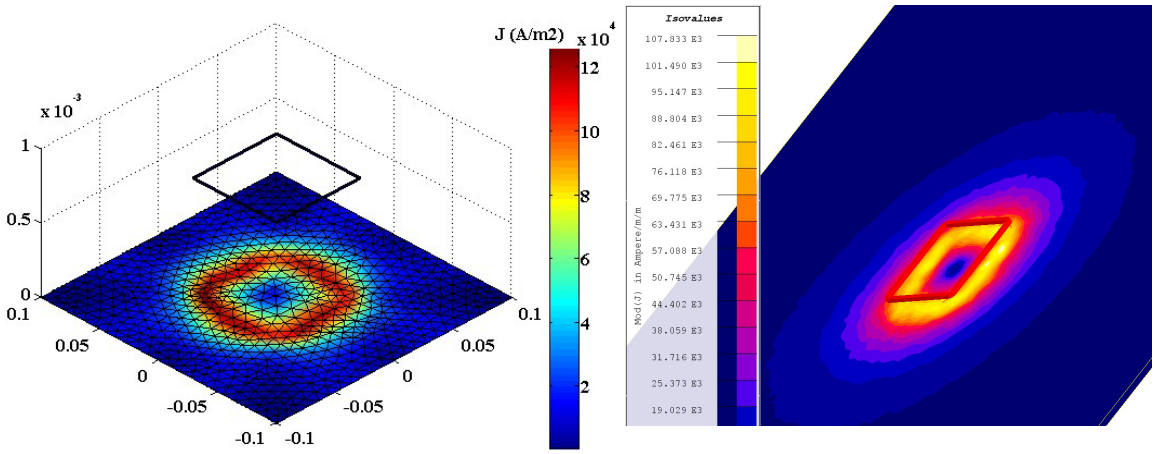

Figure 9. Eddy currents in distribution (a) FEM-PEEC method, (b) FEM.

Table 2. Comparison of the current obtained for FEM method.

Methods	Quantities		Calculation time (s) (With 0.7% difference)
	Number of elements	Eddy current value (A/m^2)	
FEM	6074	13,93 E+4	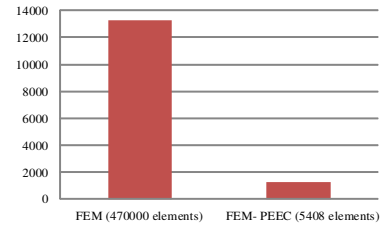
	31988	**12.80 E+4**	
FEM-PEEC	338	9.12 E+4	
	1352	11.71 E+4	
	5408	**12.71 E+4**	

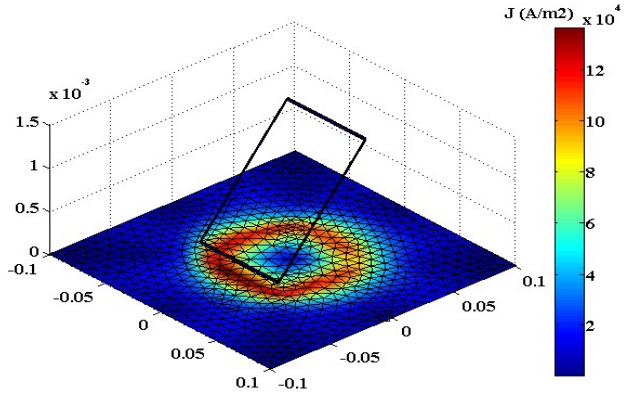

Figure 10. Coil misaligned effect on eddy current distribution.

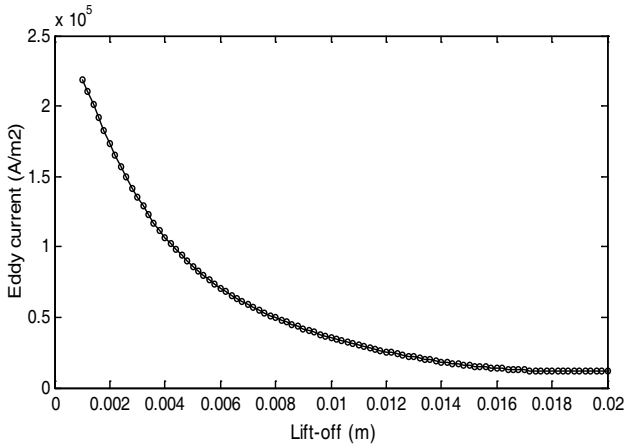

Figure 11. Lift-off effect on eddy current.

near the coil. In many applications, eddy current measurements are adversely affected by lift-off. Lift-off is considered a source of noise and is not desirable for error detection. It can be in the same direction as the crack, obscuring the crack reaction. Therefore, for a much performing NDT operation, this distance should be as constant as possible. The simulation results presented in Figure 11 have a good agreement with the physics and distance-from-source theory.

We know that the ferromagnetic substance has a good effect on the canalization of the magnetic field and consequently in the values of the eddy current. Figure 12 confirmed the good effect of magnetic permeability on eddy currents values.

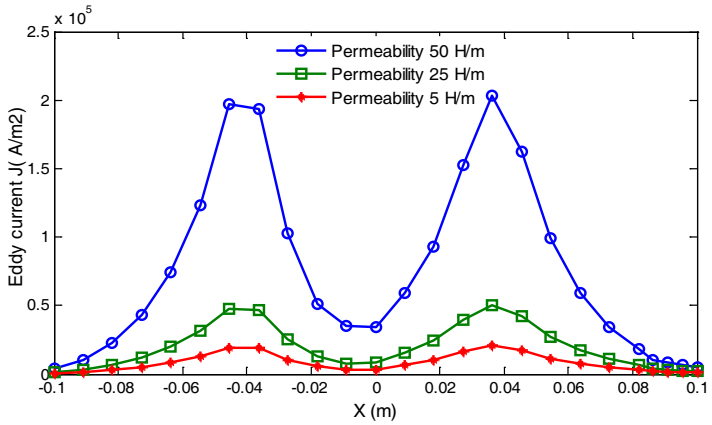

Figure 12. Magnetic permeability effect on eddy current.

5. CONCLUSION

In this study, we have developed an Integro-Differential formulation for three-dimensional eddy currents computation of structures having heterogeneous dimensions and in the vicinity of ferromagnetic substances. The proposed hybrid method also considers the impact of connection type at solid conductor's corners and inclining of coil conductor for calculating magnetic field. By PEEC method we have developed the calculation of magnetic quantities created by rectangular coil, especially the field magnetic considered as a source which generates the eddy currents in a thin plate. The first promising results have concerned the magnetic entities calculation; we have visually shown the reproduction of coil shapes through the equipotential of the magnetic field. To reduce computational effort just active regions are meshed by the FEM method. The comparison with the results obtained by FLUX3D software proves the precision and robustness leading to a significant reduction in memory requirements and computation time of our approach. Finally, we confirm that these developments have the potential to solve several difficult three dimensional electromagnetic problems that are always treated in different manners in the literature.

ACKNOWLEDGMENT

Funding was provided by the General Direction of Research and Development Technologies, Ministry of Higher Education and Research Sciences, Algeria.

REFERENCES

1. She, S., Y. Chen, Y. He, Z. Zhou, and X. Zou, "Optimal design of remote field eddy current testing probe for ferromagnetic pipeline inspection," *J. Measurement*, Vol. 168, No. 2, 108306, 2020.
2. Menana, H. and M. Feliachi, "Electromagnetic characterization of the CFRPs anisotropic conductivity: Modeling and measurements," *EPJAP*, Vol. 53, No. 2, 21101–211106, 2011.

3. Mohdeb, N., "Comparative study of circular flat spiral coils structure effect on magnetic resonance wireless power transfer performance," *Progress In Electromagnetics Research M*, Vol. 94, 119–129, 2020.
4. Wu, F., S. K. Moon, and H. Son, "Orientation measurement based on magnetic inductance by the extended distributed multi-pole model," *Sensors*, Vol. 14, 11504–11521, 2014.
5. Gendron, M., B. Hazel, E. Boudreault, H. Champliaud, and X. Pham, "Coupled thermo-electromagnetic model of a new robotic high-frequency local induction heat treatment system for large steel components," *Applied Thermal Engineering*, Vol. 150, 372–385, 2019.
6. Boudreault, E., B. Hazel, J. Côté, and S. Godin, "A new robotic process for in situ heat treatment on large steel components," *Proceedings of ASME Power Conference*, V002T06A001, Boston, Massachusetts, USA, 2013.
7. Fu, X., B. Wang, X. Zhu, X. Tang, and H. Ji, "Numerical and experimental investigations on large-diameter gear rolling with local induction heating process," *IJAMT*, Vol. 91, Nos. 1–4, 1–11, 2017.
8. Kruzík, M. and A. Prohl, "Recent developments in the modeling, analysis, and numerics of ferromagnetism," *SIAM Review*, Vol. 48, No. 3, 439–483, 2006.
9. Albertz, D., S. Dappen, and G. Henneberger, "Calculation of the 3D nonlinear eddy current field in moving conductors and its application to braking systems," *IEEE Trans. on Magnetics*, Vol. 32, No. 3, 768–771, 1996.
10. Aimé, J., B. Cogitore, G. Meunier, E. Clavel, and Y. Maréchal, "Numerical methods for eddy currents modeling of planar transformers," *IEEE Trans. on Magnetics*, Vol. 47, No. 5, 1014–1017, 2011.
11. Versaci, M., G. Angiulli, P. di Barba, and F. C. Morabito, "Joint use of eddy current imaging and fuzzy similarities to assess the integrity of steel plates," *Open Physics*, Vol. 18, No. 1, 230–240, 2020.
12. Djemoui, S., H. Allag, M. Chebout, and H. Bouchekara, "Partial electrical equivalent circuits and finite difference methods coupling; application to eddy currents calculation for conductive and magnetic thin plates," *Progress In Electromagnetics Research C*, Vol. 114, 83–96, 2021.
13. Allag, H., J.-P. Yonnet, M. Fassenet, and M. E. H. Latreche, "3D analytical calculation of interactions between perpendicularly magnetized magnets — Application to any magnetization direction," *Sensor Letters*, Vol. 7, No. 3, 486–491, 2009.
14. Albanese, R., G. Rubinacci, A. Tamburrino, S. Ventre, and F. Villone, "A fast 3D eddy current integral formulation," *COMPEL*, Vol. 20, No. 2, 317–331, 2001.
15. Chebout, M., H. Azizi, and M. R. Mekideche, "A model assisted probability of detection approach for ecndt of hidden defect in aircraft structures," *Progress In Electromagnetics Research Letters*, Vol. 95, 1–8, 2021.
16. Simkin, J. and C. W. Trowbridge, "On the use of the total scalar potential in the numerical solution of field problem in electromagnetics," *International Journal in the Numerical Methods in Engineering*, Vol. 14, 423–440, 1979.
17. Le-Duc, T., G. Meunier, O. Chadebec, and J.-M. Guichon, "A new integral formulation for eddy current computation in thin conductive shells," *IEEE Trans. on Magnetics*, Vol. 48, No. 2, 427–430, 2012.
18. Chadebec, O., J. L. Coulomb, and F. Janet, "A review of magnetostatic moment method," *IEEE Tran. on Magnetics*, Vol. 42, No. 4, 515–520, 2006.
19. Kruzík, M., and A. Prohl, "Recent developments in the modeling, analysis, and numerics of ferromagnetism," *SIAM Review*, Vol. 48, No. 3, 439–483, 2006.
20. Albertz, D., S. Dappen, and G. Henneberger, "Calculation of the 3D nonlinear eddy current field in moving conductors and its application to braking systems," *IEEE Trans. on Magnetics*, Vol. 32, No. 3, 768–771, 1996.
21. Zarko, D., S. Stipetic, M. Martinovic, M. Kovacic, T. Jercic, and Z. Hanic, "Reduction of computational efforts in finite element based permanent magnet traction motor optimization,"

IEEE Transactions on Industrial Electronics, Vol. 65, No. 2, 1799–1807, 2018.

22. Aomar, L., H. Allag, M. Feliachi, and J. P. Yonnet, "3-D integral approach for calculating mutual interactions between polygon-shaped massive coils," *IEEE Trans. on Magnetics*, Vol. 53, No. 11, 1–5, 2017.
23. Allag, H. and J.-P. Yonnet, "3-D analytical calculation of the torque and force exerted between two cuboidal magnets," *IEEE Trans. on Magnetics*, Vol. 45, No. 10, 3969–3972, 2009.
24. Allag, H., J.-P. Yonnet, and M. E. H. Latreche, "Analytical calculation of the torque exerted between two perpendicularly magnetized magnets," *Journal of Applied Physics*, Vol. 109, No. 7, 07E701, 2011.
25. Babic, S. and C. Akyel, "New formulas for mutual inductance and axial magnetic force between magnetically coupled coils: Thick circular coil of the rectangular cross-section-thin disk coil (Pancake)," *IEEE Trans. on Magnetics*, Vol. 49, No. 2, 860–868, 2013.
26. Ekman, J., G. Antonini, A. Orlandi, and A. E. Ruehli, "Stability of PEEC models with respect to partial element accuracy," *Symposium on EMC*, Vol. 1, 271–276, Santa Clara, California, USA, 2004.
27. Ruehli, A. E., "Inductance calculations in a complex integrated circuit environment," *IBM Journal of Research and Development*, Vol. 16, No. 5, 470–481, 1972.
28. Antonini, G., D. Deschrijver, and T. Dhaene, "Broadband macromodels for retarded partial element equivalent circuit (rPEEC) method," *IEEE Trans. EMC*, Vol. 49, 35–48, 2007.
29. Babic, S. and C. Akyel, "New formulas for mutual inductance and axial magnetic force between magnetically coupled coils: Thick circular coil of the rectangular cross-section-thin disk coil (Pancake)," *IEEE Trans. on Magnetics*, Vol. 49, No. 2, 860–868, 2013.
30. Ekman, J., G. Antonini, A. Orlandi, and A. E. Ruehli, "Stability of PEEC models with respect to partial element accuracy," *Symposium on EMC*, Vol. 1, 271–276, Santa Clara, California, USA, 2004.
31. Ruehli, A. E., G. Antonini, and L. Jiang, *Circuit Oriented Electromagnetic Modeling Using the PEEC Techniques*, Wiley & Sons, Inc., Hoboken, New Jersey, USA, 2017.
32. Kwon, O. M., M. V. K. Chari, S. J. Salon, and K. Sivasubramaniam, "Development of integral equation solution for 3-D eddy current distribution in a conducting body," *IEEE Tran. on Magnetics*, Vol. 39, No. 5, 2612–2614, 2003.
33. Kriezis, E. E., T. D. Tsiboukis, S. M. Panas, and J. A. Tegopoulos, "Eddy currents: Theory and applications," *Proceeding of the IEEE*, Vol. 80, No. 10, 1559–1589, 1992.